

Inversion of Methane on Transition-Metal Complexes: A Possible Mechanism for Inversion of Stereochemistry

Kazunari Yoshizawa,^{*,†} Akiya Suzuki, and Tokio Yamabe

Contribution from the Department of Molecular Engineering, Kyoto University, Sakyo-ku, Kyoto 606-8501, Japan, and Institute for Fundamental Chemistry, 34-4 Takano-Nishihiraki-cho, Sakyo-ku, Kyoto 606-8103, Japan

Received November 12, 1998. Revised Manuscript Received March 15, 1999

Abstract: The inversion of methane bound to first-row transition-metal ions from Sc⁺ to Cu⁺ is systematically investigated using the B3LYP method, a hybrid density-functional-theory method of Becke and Lee, Yang, and Parr. The computed transition states for the methane inversion on the M⁺(CH₄) complexes have a C_s structure in which one pair of C–H bonds is about 1.2 Å in length and the other pair is about 1.1 Å. The barrier height for the methane inversion is significantly decreased from 109 kcal/mol for free methane to 43–48 kcal/mol on the late transition-metal complexes, Fe⁺(CH₄), Co⁺(CH₄), Ni⁺(CH₄), and Cu⁺(CH₄). Since each activation energy involves the binding energy of the complex (16 kcal/mol on the average), the actual barrier height should be lower by this quantity if measured from the dissociation limit. The inversion of methane can therefore occur at the transition-metal active center of catalysts or enzymes under ambient conditions through a thermally accessible transition state, and it would reasonably lead to inversion of stereochemistry at a carbon atom in catalytic reactions of hydrocarbons. We propose that a radical mechanism based on a planar carbon species may not be the sole source of the observed loss of stereochemistry in transition-metal-catalyzed hydrocarbon hydroxylations and other related reactions.

Introduction

In 1970, Hoffmann, Alder, and Wilcox¹ suggested the transformation of tetrahedral to planar methane through a symmetry-allowed process for either a twisting ($T_d \rightarrow D_2 \rightarrow D_{4h}$) or a squashing ($T_d \rightarrow D_{2d} \rightarrow D_{4h}$) pathway. Their extended Hückel² calculations told us that T_d methane is more stable than D_{4h} methane with identical bond lengths of 1.10 Å by 127 kcal/mol. CNDO³ and approximate ab initio Hartree–Fock (HF)⁴ calculations yielded 187 and 249 kcal/mol, respectively, for the same quantity. The results of this investigation have stimulated experimental and further theoretical studies. The synthesis of compounds containing a planar-tetracoordinate carbon (the so-called “anti van’t Hoff/LeBel structure”) that are stable enough to be isolated and characterized under ambient conditions has continued to be a challenging target.⁵ More recent intensive calculations, by Collins et al.,⁶ afforded 240 kcal/mol at the HF/STO-3G level of theory,⁷ 168 kcal/mol at the HF/4-31G

level,⁸ 171 kcal/mol at the HF/6-31G* level,⁹ and 160 kcal/mol at the MP2/6-31G* level.¹⁰ Crans and Snyder¹¹ predicted from MNDO¹² and PRDDO¹³-GVB¹⁴ calculations using a multiconfigurational wave function that the open-shell singlet state of ¹B_{2u} symmetry should lie 25–30 kcal/mol below the closed-shell ¹A_g state.

Calculated normal-mode vibrational frequencies play an essential role in the characterization of a molecular potential energy hypersurface. Unfortunately, no vibrational analysis was carried out until recently for the supposed D_{4h} transition state for the inversion of methane. In 1993 Gordon and Schmidt¹⁵ demonstrated from detailed analyses of Hessians (matrix of energy second derivatives) that the D_{4h} square planar structure is not a true transition state for the inversion of methane. It was found from detailed vibrational analyses that the closed-shell ¹A_g state with a D_{4h} structure has three imaginary vibrational modes of B_{2u}, A_{2u}, and E_u symmetry, and the open-shell ¹B_{2u} state also has two imaginary modes of B_{2u} and B_{1g} symmetry. Since a true transition state, a saddle point on a potential energy surface, should have only one imaginary mode of vibration, these singlet states with D_{4h} structures are not a transition state.

The true inversion transition state was found to have a distorted C_s structure,¹⁵ being quite different both geometrically and energetically from the previously presumed square-planar

[†] To whom all correspondence should be addressed at Kyoto University. E-mail: kazunari@scl.kyoto-u.ac.jp.

(1) (a) Hoffmann, R.; Alder, R. W.; Wilcox, C. F., Jr. *J. Am. Chem. Soc.* **1970**, *92*, 4992. (b) A recent, related paper: Radius, U.; Silverio, S. J.; Hoffmann, R.; Gleiter, R. *Organometallics* **1996**, *15*, 3737.

(2) (a) Hoffmann, R. *J. Chem. Phys.* **1963**, *39*, 1397. (b) Hoffmann, R.; Lipscomb, W. N. *J. Chem. Phys.* **1962**, *36*, 2179; *37*, 2872.

(3) (a) Pople, J. A.; Santry, D. P.; Segal, G. A. *J. Chem. Phys.* **1965**, *43*, S129. (b) Pople, J. A.; Segal, G. A. *J. Chem. Phys.* **1965**, *43*, S136. (c) Pople, J. A.; Segal, G. A. *J. Chem. Phys.* **1966**, *44*, 3289.

(4) Monkhorst, H. *J. Chem. Commun.* **1968**, 111.

(5) (a) van't Hoff, J. H. *Arch. Neerl. Sci. Exactes Nat.* **1874**, 445. (b) LeBel, J. A. *Bull. Soc. Chim. Fr.* **1874**, *22*, 337. Review: (c) Röttger, D.; Erker, G. *Angew. Chem., Int. Ed. Engl.* **1997**, *36*, 812.

(6) (a) Collins, J. B.; Dill, J. D.; Jemmis, E. D.; Apeloig, Y.; Schleyer, P. v. R.; Seeger, R.; Pople, J. A. *J. Am. Chem. Soc.* **1976**, *98*, 5419. (b) Krogh-Jespersen, M.-B.; Chandrasekhar, J.; Würthwein, E.-U.; Collins, J. B.; Schleyer, P. v. R. *J. Am. Chem. Soc.* **1980**, *102*, 2263.

(7) Hehre, W. J.; Stewart, R. F.; Pople, J. A. *J. Chem. Phys.* **1969**, *51*, 2657.

(8) Ditchfield, R.; Hehre, W. J.; Pople, J. A. *J. Chem. Phys.* **1971**, *54*, 724.

(9) Hariharan, P. C.; Pople, J. A. *Theor. Chim. Acta* **1973**, *28*, 213.

(10) Binkley, J. S.; Pople, J. A. *Int. J. Quantum Chem.* **1975**, *9*, 229.

(11) Crans, D. C.; Snyder, J. P. *J. Am. Chem. Soc.* **1980**, *102*, 7152.

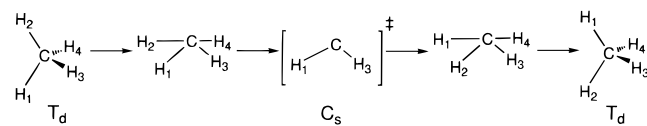
(12) Dewar, M. J. S.; Thiel, W. *J. Am. Chem. Soc.* **1977**, *99*, 4899.

(13) Halgren, T. A.; Lipscomb, W. N. *J. Chem. Phys.* **1973**, *58*, 1569.

(14) Goddard, W. A.; Dunning, T. H.; Hunt, W.; Hay, P. *J. Acc. Chem. Res.* **1973**, *6*, 368.

(15) Gordon, M. S.; Schmidt, M. W. *J. Am. Chem. Soc.* **1993**, *115*, 7486.

Scheme 1



D_{4h} saddle point. The movement of the H atoms of methane along the reaction coordinate is complicated, as indicated in Scheme 1. This transition state is 125.6, 117.9, and 117.0 kcal/mol higher in energy than the global minimum of the T_d structure at the MCSCF/TZV++G(d,p), SOCI/TZV++G(d,p), and SOCI/TZV++G(d,p) with Davidson correction levels of theory, respectively.¹⁵ Since this barrier height is larger than the C–H bond dissociation energy of 104 kcal/mol, methane is unlikely to undergo such interesting inversion under ambient conditions. The C_s transition state exhibits a rather strange pyramidal structure that we cannot intuitively imagine; one pair of C–H bonds is computed to be 1.316 Å in length and the other pair 1.131 Å.

On the activation of the C–H bonds of small alkanes, there has been considerable experimental¹⁶ and theoretical¹⁷ work. Alkane or methane complexes are proposed to be possible intermediates involved in C–H bond activation reactions. Since the C–H bonds of methane can be weakened on transition-metal complexes, we consider that the barrier height of the methane inversion should be significantly decreased if the

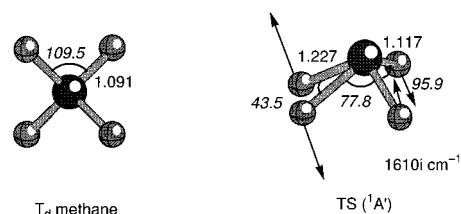


Figure 1. Geometries of the T_d global minimum and the C_s transition state for the inversion of free methane. The bond distances are in angstroms, and the bond angles (italic) are in degrees. The arrows in the transition state indicate the transition vector.

inversion occurs on a methane σ -complex. The purpose of our work is to investigate whether the inversion of methane occurs reasonably well at the transition-metal active center under ambient conditions through a thermally accessible, low-lying transition state. We will answer with a “yes” in respect of this question. On the basis of the mechanism which is a concerted process, we will give an alternative explanation for the inversion of stereochemistry at a carbon atom observed in catalytic reactions of hydrocarbons.

Results and Discussion

Inversion of Free Methane. We first reproduce the true transition state as well as the reaction pathway for the inversion of free methane with the B3LYP method of Becke¹⁸ and Lee, Yang, and Parr,¹⁹ a hybrid (density-functional-theory/Hartree–Fock) method. The preparative computations are necessary for us to have a better understanding of the interesting inversion of methane at the transition-metal active center because the transition-state structure and the reaction pathway are somewhat complicated, as mentioned above. This also seems a good test for the performance of this popular density-functional-theory (DFT) method. A detailed description of our computations will be given later in this paper. From B3LYP computations, it was shown that the closed-shell 1A_g state with a planar D_{4h} structure also has three imaginary vibrational modes and that the $^1A'$ state with a C_s structure has only one imaginary mode. The C_s transition state was computed to lie 21.4 kcal/mol below the D_{4h} methane. Let us briefly discuss the geometry change and the reaction pathway of the inversion via the C_s methane. Figure 1 shows optimized geometries for the T_d global minimum and the C_s transition state of methane, in which the imaginary mode of vibration is indicated for the transition state. Since we found only one imaginary mode of $1610i\text{ cm}^{-1}$ for this C_s structure, this corresponds to the true transition state for the inversion of methane. The imaginary mode in the transition state indicates nuclear motions along the preferred reaction pathway. One pair of C–H bonds of the C_s transition state is 1.227 Å in length, and the other pair is 1.117 Å. The bond angle of H–C–H for the long C–H pair is 43.5° , and that for the short C–H pair is 95.9° . The activation barrier for this transition state was computed with zero point vibrational energy corrections to be 109.4 kcal/mol. This barrier height is a little larger than the energy that is required to break a C–H bond of methane (104 kcal/mol). These B3LYP DFT computational results are thus in quantitative agreement with the earlier high-level, multiconfigurational analyses of Gordon and Schmidt.¹⁵

The energy profile and the geometrical change along the intrinsic reaction coordinate (IRC)²⁰ for the inversion of methane

(18) (a) Becke, A. D. *Phys. Rev.* **1988**, A38, 3098. (b) Becke, A. D. *J. Chem. Phys.* **1993**, 98, 5648.

(19) Lee, C.; Yang, W.; Parr, R. G. *Phys. Rev.* **1988**, B37, 785.

(20) (a) Fukui, K. *J. Phys. Chem.* **1970**, 74, 4161. (b) Fukui, K. *Acc. Chem. Res.* **1981**, 14, 363.

(16) (a) Shilov, A. E. *Metal Complexes in Biomimetic Chemical Reactions*; CRC: Boca Raton, 1996. (b) Shilov, A. E.; Shul'pin, G. B. *Chem. Rev.* **1997**, 97, 2879. (c) Bergman, R. G. *Science* **1984**, 223, 902. (d) Arndtsen, B. A.; Bergman, R. G.; Mobley, T. A.; Peterson, T. H. *Acc. Chem. Res.* **1995**, 28, 154. (e) Hill, C. L., Ed. *Activation and Functionalization of Alkanes*; Wiley: New York, 1989. (f) Davies, J. A.; Watson, P. L.; Liebman, J. F.; Greenberg, A. *Selective Hydrocarbon Activation*; VCH: New York, 1990. (g) Crabtree, R. H. *Chem. Rev.* **1985**, 85, 245. (h) Crabtree, R. H. *Chem. Rev.* **1995**, 95, 987. (i) Barton, D. H. R.; Doller, D. *Acc. Chem. Res.* **1992**, 25, 504. (j) Alexander, D. R. *Chem. Rev.* **1990**, 97, 403. (k) Hall, C.; Perutz, R. N. *Chem. Rev.* **1996**, 96, 3125. (l) Gesser, H. D.; Hunter, N. R.; Prakash, C. B. *Chem. Rev.* **1985**, 85, 237. (m) Schröder, D.; Schwarz, H. *Angew. Chem., Int. Ed. Engl.* **1995**, 34, 1973.

(17) (a) Saillard, J.-Y.; Hoffmann, R. *J. Am. Chem. Soc.* **1984**, 106, 2006. (b) Perry, J. K.; Ohanessian, G.; Goddard, W. A., III. *J. Phys. Chem.* **1993**, 97, 5238. (c) Perry, J. K.; Ohanessian, G.; Goddard, W. A., III. *Organometallics* **1994**, 13, 1870. (d) Blomberg, M. R. A.; Siegbahn, P. E. M.; Svensson, M. *J. Am. Chem. Soc.* **1992**, 114, 6095. (e) Siegbahn, P. E. M.; Blomberg, M. R. A. *Organometallics* **1994**, 13, 354. (f) Siegbahn, P. E. M. *Organometallics* **1994**, 13, 2833. (g) Siegbahn, P. E. M. *J. Am. Chem. Soc.* **1996**, 118, 1487. (h) Siegbahn, P. E. M.; Crabtree, R. H. *J. Am. Chem. Soc.* **1996**, 118, 4442. (i) Ziegler, T.; Tschinke, V.; Becke, A. D. *J. Am. Chem. Soc.* **1987**, 109, 1351. (j) Ziegler, T.; Tschinke, V.; Fan, L.; Becke, A. D. *J. Am. Chem. Soc.* **1989**, 111, 9177. (k) Ziegler, T.; Folga, E.; Berces, A. *J. Am. Chem. Soc.* **1993**, 115, 636. (l) Koga, N.; Morokuma, K. *J. Phys. Chem.* **1990**, 94, 5454. (m) Musaev, D. G.; Koga, N.; Morokuma, K. *J. Phys. Chem.* **1993**, 97, 4064. (n) Musaev, D. G.; Morokuma, K.; Koga, N.; Nguyen, K.; Gordon, M. S.; Cundari, T. R. *J. Phys. Chem.* **1993**, 97, 11435. (o) Musaev, D. G.; Morokuma, K. *J. Chem. Phys.* **1994**, 101, 10697. (p) Musaev, D. G.; Morokuma, K. *J. Phys. Chem.* **1996**, 100, 11600. (q) Sakaki, S.; Ieki, M. *J. Am. Chem. Soc.* **1991**, 113, 5063. (r) Sakaki, S.; Ieki, M. *J. Am. Chem. Soc.* **1993**, 115, 2373. (s) Cundari, T. R. *J. Am. Chem. Soc.* **1992**, 114, 10557. (t) Cundari, T. R. *J. Am. Chem. Soc.* **1994**, 116, 340. (u) Schröder, D.; Fiedler, A.; Hrušák, J.; Schwarz, H. *J. Am. Chem. Soc.* **1992**, 114, 1215. (v) Fiedler, A.; Hrušák, J.; Koch, W.; Schwarz, H. *Chem. Phys. Lett.* **1993**, 211, 242. (w) Fiedler, A.; Schröder, D.; Shaik, S.; Schwarz, H. *J. Am. Chem. Soc.* **1994**, 116, 10734. (x) Wesendrup, R.; Schalley, C. A.; Schröder, D.; Schwarz, H. *Chem. Eur. J.* **1995**, 1, 608. (y) Shaik, S.; Danovich, D.; Fiedler, A.; Schröder, D.; Schwarz, H. *Helv. Chim. Acta* **1995**, 78, 1393. (z) Ryan, M. F.; Fiedler, A.; Schröder, D.; Schwarz, H. *J. Am. Chem. Soc.* **1995**, 117, 2033. (aa) Holthausen, M. C.; Fiedler, A.; Schwarz, H.; Koch, W. *J. Phys. Chem.* **1996**, 100, 6236. (bb) Fiedler, A.; Schröder, D.; Schwarz, H.; Tjelta, B. L.; Armentrout, P. B. *J. Am. Chem. Soc.* **1996**, 118, 5047. (cc) Holthausen, M. C.; Koch, W. *Helv. Chim. Acta* **1996**, 79, 1939. (dd) Holthausen, M. C.; Koch, W. *J. Am. Chem. Soc.* **1996**, 118, 9932. (ee) Holthausen, M. C.; Hornung, G.; Schröder, D.; Sen, S.; Koch, W.; Schwarz, H. *Organometallics* **1997**, 16, 3135. (ff) Sändig, N.; Koch, W. *Organometallics* **1997**, 16, 5242.

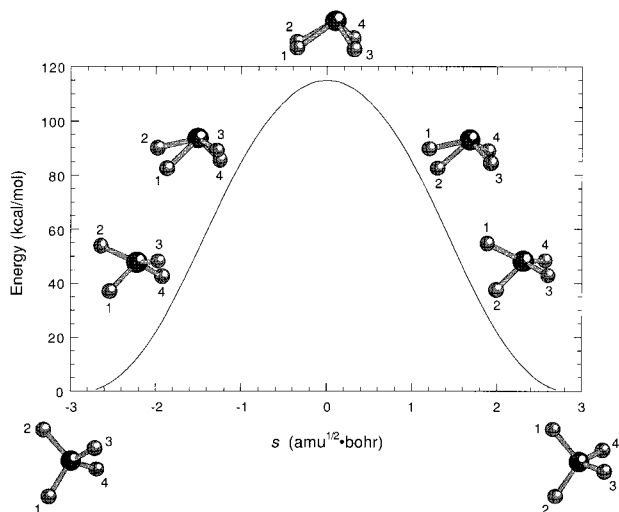


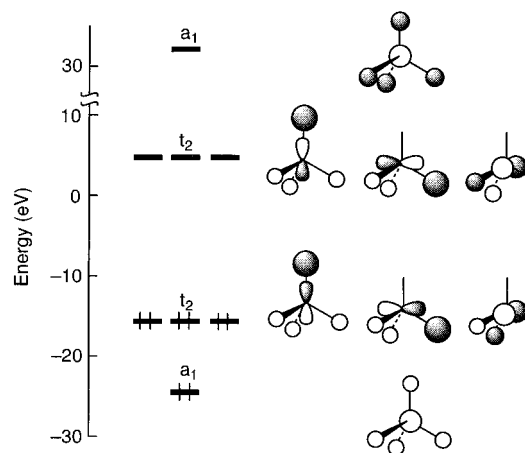
Figure 2. Energy profile and geometrical change along the intrinsic reaction coordinate (IRC) for the inversion of free methane. Corrections of zero point vibrational energy are not included in the IRC analysis.

are shown in Figure 2. Note that the barrier height in this illustration is not exactly 109.4 kcal/mol since zero point vibrational energy corrections are not included in the IRC analysis. It is essential to understand the complicated movement of H atoms that leads to the inversion of methane via the C_s transition state. The present IRC profile is, of course, consistent with the previous one propounded at a higher level of theory.¹⁵ Thus, we are able to reasonably derive excellent descriptions of the inversion of methane from B3LYP DFT computations, particularly in the molecular geometries, the reaction pathway, and the activation energy of the transition state. The method of choice is therefore appropriate for the issue of this paper.

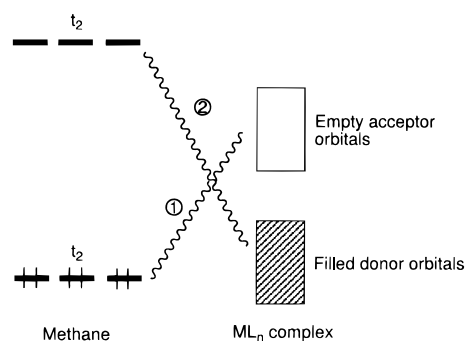
Methane Inversion at Transition Metals. Having described the inversion of free methane, let us consider in this section how differently the inversion of methane proceeds at the transition-metal active center. As mentioned above, alkane complexes are accepted intermediates proposed to be involved in C–H bond activation reactions. The binding of methane to Sc^+ , Fe^+ , Co^+ , Rh^+ , and Ir^+ has been theoretically studied by Morokuma and collaborators.^{17m–p} Recently, related methane complexes have been extensively investigated using modern spectroscopic techniques.²¹ Low-temperature photolysis of CH_3CoH to give the σ -complex, $Co(CH_4)$, was reported by Billups et al.;²¹ their FTIR matrix isolation spectroscopy in solid argon demonstrated that the methane is significantly distorted on the cobalt complex. It is therefore of general interest to consider whether the inversion of methane reasonably occurs at the transition-metal active center of the complex. Our main purpose of this paper is to study whether the barrier height is decreased from the value for free methane so that it could serve as a thermally accessible, low-lying transition state.

Before we present DFT computational results, it would be useful to consider the activation of methane from a point of

Scheme 2



Scheme 3



view of its molecular orbitals. The molecular orbitals of methane from an extended Hückel² calculation are indicated in Scheme 2. It is essential for our discussion presented below to note that the 3-fold degenerate t_2 HOMO is C–H bonding (in-phase) and that the t_2 LUMO is C–H antibonding (out-of-phase). The HOMO–LUMO gap is about 20 eV, and therefore methane is a very hard hydrocarbon with unusually strong C–H bonds. In view of these frontier orbitals, the C–H bonds of methane can be weakened when the LUMO is partly filled or the HOMO is partly unfilled as a result of electron transfer or orbital interaction with other molecules, particularly with transition-metal complexes.

As indicated in Scheme 3, the C–H bonds of methane are activated on transition-metal complexes because of both the electron transfer from the methane t_2 HOMO to the unfilled d-block orbitals of complex ① and the electron transfer from the filled d-block orbitals to the methane t_2 LUMO ②. This schematic representation has been successfully used in describing the activation of methane and dihydrogen on both discrete transition-metal complexes and transition-metal surfaces.^{17a} On the basis of this qualitative picture, we have discussed the activation of methane and its conversion to methanol on the diiron active site of soluble methane monooxygenase (MMO).²² We can expect that the formation of a methane σ -complex should result in a small activation energy for the inversion of methane because the C–H bonds of methane are weakened as a consequence of the orbital interactions. Our qualitative prediction is quite reasonable from a theoretical viewpoint. Clearly, ab initio computations are necessary for quantitative

(21) (a) Trevor, D. J.; Cox, D. M.; Kaldor, A. *J. Am. Chem. Soc.* **1990**, *112*, 3742. (b) Irikura, K. K.; Beauchamp, J. L. *J. Phys. Chem.* **1991**, *95*, 8344. (c) Ranasinghe, Y. A.; MacMahon, T. J.; Freiser, B. S. *J. Phys. Chem.* **1991**, *95*, 7721. (d) Van Zee, R. J.; Li, S.; Weltner, W., Jr. *J. Am. Chem. Soc.* **1993**, *115*, 2976. (e) Carrol, J. J.; Weisshaar, J. C. *J. Am. Chem. Soc.* **1993**, *115*, 800. (f) Burger, P.; Bergman, R. G. *J. Am. Chem. Soc.* **1993**, *115*, 10462. (g) Schaller, C. P.; Bonanno, J. B.; Wolczanski, P. T. *J. Am. Chem. Soc.* **1994**, *116*, 4133. (h) Zhang, X.-X.; Wayland, B. B. *J. Am. Chem. Soc.* **1994**, *116*, 7897. (i) Billups, W. E.; Chang, S.-C.; Hauge, R. H.; Margrave, J. L. *J. Am. Chem. Soc.* **1995**, *117*, 1387. (j) van Koppen, P. A. M.; Kemper, P. R.; Bushnell, J. E.; Bowers, M. T. *J. Am. Chem. Soc.* **1995**, *117*, 2098. (k) Campbell, M. L. *J. Am. Chem. Soc.* **1997**, *119*, 5984.

(22) (a) Yoshizawa, K. *J. Biol. Inorg. Chem.* **1998**, *3*, 318. (b) Yoshizawa, K.; Hoffmann, R. *Inorg. Chem.* **1996**, *35*, 2409. (c) Yoshizawa, K.; Yamabe, T.; Hoffmann, R. *New J. Chem.* **1997**, *21*, 151. (d) Yoshizawa, K.; Ohta, T.; Yamabe, T.; Hoffmann, R. *J. Am. Chem. Soc.* **1997**, *119*, 12311.

Table 1. Computed Barrier Heights (in kcal/mol) for the Inversion of Methane on the $M^+(\text{CH}_4)$ Complexes, in Which M^+ Is the First-Row Transition-Metal Ions. The Values Indicated Are Measured from the $M^+(\text{CH}_4)$ Complexes, and Actual Barrier Heights Should Be 16 kcal/mol Lower on the Average If Measured from the Reactants. The Symmetry Labels Indicated Are for the Transition States

complex	low spin	high spin	complex	low spin	high spin
Sc ⁺ (CH ₄)	64.1 (¹ A')	64.8 (³ A')			
Ti ⁺ (CH ₄)	58.8 (² A')	55.4 (⁴ A')	Fe ⁺ (CH ₄)	47.9 (⁴ A')	59.2 (⁶ A')
V ⁺ (CH ₄)	64.6 (³ A')	65.1 (⁵ A')	Co ⁺ (CH ₄)	46.0 (³ A')	59.0 (⁵ A')
Cr ⁺ (CH ₄)	52.3 (⁴ A')	58.3 (⁶ A')	Ni ⁺ (CH ₄)	48.4 (² A')	55.9 (⁴ A')
Mn ⁺ (CH ₄)	53.2 (⁵ A')	65.5 (⁷ A')	Cu ⁺ (CH ₄)	47.9 (¹ A')	43.1 (³ A')

Table 2. Computed Total Charges of Methane in the Reactants and the Transition States. Values in Parentheses Are for the Transition States

complex	low spin	high spin	complex	low spin	high spin
Sc ⁺ (CH ₄)	0.13 (0.27)	0.11 (0.19)	Fe ⁺ (CH ₄)	0.08 (0.26)	0.07 (0.20)
Ti ⁺ (CH ₄)	0.11 (0.21)	0.09 (0.20)	Co ⁺ (CH ₄)	0.02 (0.25)	0.07 (0.21)
V ⁺ (CH ₄)	0.10 (0.20)	0.07 (0.20)	Ni ⁺ (CH ₄)	0.06 (0.18)	0.09 (0.24)
Cr ⁺ (CH ₄)	0.10 (0.25)	0.06 (0.20)	Cu ⁺ (CH ₄)	0.04 (0.22)	0.07 (0.30)
Mn ⁺ (CH ₄)	0.11 (0.26)	0.05 (0.16)			

discussion on the inversion of methane on a σ -complex through a low-lying transition state.

We carried out systematic B3LYP computations on the $M^+(\text{CH}_4)$ σ -complexes and the transition states for the inversion of methane on the complexes, in which M^+ is a first-row transition-metal ion from Sc⁺ to Cu⁺. Computed values of the activation energy for the inversion of methane on the $M^+(\text{CH}_4)$ σ -complexes are listed in Table 1. As we expected, the activation energy is significantly decreased from 109 kcal/mol for free methane to less than 50 kcal/mol in some of the spin states of the methane complexes. These values, of course, include zero point vibrational energy corrections. Note that the low-spin states of the late transition-metal ions and the high-spin state of the Cu⁺ ion afford small values of less than 50 kcal/mol. It is 43–48 kcal/mol on the Fe⁺(CH₄), Co⁺(CH₄), Ni⁺(CH₄), and Cu⁺(CH₄) complexes. It seems to us that these activation energies would still require high temperatures for the inversion of methane to be facile. It is our concern whether such low-lying transition states are thermally accessible or not. Since each activation energy indicated in Table 1 involves the binding energy of the $M^+(\text{CH}_4)$ complex (16 kcal/mol on the average), the actual barrier height should be lower by this quantity if measured from the dissociation limit, i.e., the transition-metal ion and methane. Moreover, we think that the kinetic energy that the reactants initially possess can in part overcome the activation barrier. Thus, we think that the transition states should be thermally accessible.

Computed values of the total charge of methane are listed in Table 2. The charge transfer in the $M^+(\text{CH}_4)$ complexes is not so large, but this result is a clear indication of methane activation on the σ -complexes. The activation energies seem to be small when the amount of apparent charge transfer is small on the σ -complexes. In the early transition-metal ions, donation from the metal to the methane is unlikely to play a role and back-donation from the methane to the metal is dominant, and as a result the total charge of methane is large. On the other hand, in the late transition-metal ions, both donation from the metal and back-donation from the methane are operative, and therefore the total charge of methane is small, due to cancellation. As a consequence, the methane on the $M^+(\text{CH}_4)$ complexes becomes rather "soft" compared to free methane especially on the late transition-metal complexes, due to both the donor and the

Scheme 4

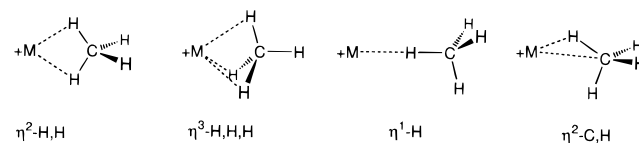


Table 3. Computed M–C Distances (in Å) of the Reactant Complex $M^+(\text{CH}_4)$ and Energy Differences (in kcal/mol) between the High-Spin and Low-Spin States. A Plus Value in the Energy Difference, $\Delta E = E(\text{HS}) - E(\text{LS})$, Means That the Low-Spin State Is the Ground State

complex	low spin	high spin	ΔE
Sc ⁺ (CH ₄)	2.210 (η^2 , nearly C_{3v})	2.425 (η^3 , nearly C_{3v})	−10.7
Ti ⁺ (CH ₄)	2.456 (in between η^2 and η^3)	2.278 (η^3 , nearly C_{3v})	−4.2
V ⁺ (CH ₄)	2.456 (η^2 , nearly C_{2v})	2.472 (η^2 , C_{2v})	−18.4
Cr ⁺ (CH ₄)	2.354 (η^2 , nearly C_{2v})	2.404 (η^2 , C_{2v})	−34.4
Mn ⁺ (CH ₄)	2.299 (η^3 , nearly C_{3v})	2.768 (η^3 , nearly C_{3v})	−13.4
Fe ⁺ (CH ₄)	2.373 (η^2 , C_{2v})	2.780 (η^2 , C_{2v})	0.2
Co ⁺ (CH ₄)	2.223 (η^2 , C_{2v})	2.633 (η^3 , nearly C_{3v})	9.2
Ni ⁺ (CH ₄)	2.204 (η^2 , C_{2v})	2.613 (η^2 -C,H)	14.2
Cu ⁺ (CH ₄)	2.083 (η^2 , C_{2v})	2.590 (η^3 , nearly C_{3v})	60.3

acceptor interactions indicated in Scheme 3. Clearly, the charge transfers or the orbital interactions result in the small values of methane inversion energy listed in Table 1. We therefore expect that the inversion of methane and alkanes should reasonably occur at the transition-metal active center of a σ -complex.

We next look at optimized structures of the reactant (= product) and the transition state for the inversion of methane on the $M^+(\text{CH}_4)$ complexes. There are, in general, two kinds of preferred binding modes for methane, the η^2 -H,H and η^3 -H,H,H modes indicated in Scheme 4. Although we do not show a dotted line between the carbon atom and the M^+ ion, this interaction is found from orbital interaction analyses to be more dominant than that between a hydrogen atom and the M^+ ion in the two binding modes. The η^1 -H and η^2 -C,H modes indicated in Scheme 4 are rare. It is of general interest to systematically investigate which binding mode is energetically preferred in such methane complexes.^{17m-p} As mentioned above, most of the methane complexes investigated take η^2 -H,H and η^3 -H,H,H modes, as listed in Table 3. It is difficult to derive a reasonable conclusion from the present computational results in respect to preferred binding mode, but the low-spin states are likely to prefer the η^2 -H,H mode and the high-spin states the η^3 -H,H,H mode. The doublet state of the Ti⁺(CH₄) complex prefers an intermediate between the η^2 -H,H and η^3 -H,H,H modes, and the quartet state of the Ni⁺(CH₄) complex prefers an η^2 -C,H mode. Computed values of energy difference ($\Delta E = E(\text{HS}) - E(\text{LS})$) between the high-spin and low-spin states of the $M^+(\text{CH}_4)$ complexes are also listed in Table 3. The high-spin states are preferred in the early transition-metal complexes whereas the low-spin states are more stable in the late transition-metal complexes.

Let us next look in detail at the Fe⁺ complex. Our B3LYP computations demonstrate that the Fe⁺(CH₄) complex exhibits η^2 -H,H binding modes in both spin states, as shown in Figure 3. The H–C–H angle near the Fe⁺ ion was computed to be approximately 116° in both spin states of the Fe⁺(CH₄) complex. This structure is significantly stabilized by both the donor and the acceptor interactions in Scheme 3. The Fe–C distance of the reactant (or product) complex is 2.373 Å in the quartet state and 2.780 Å in the sextet state, being in line with a general feature of transition-metal complexes, namely, that the metal–ligand distance in a high-spin state is longer than that in a low-

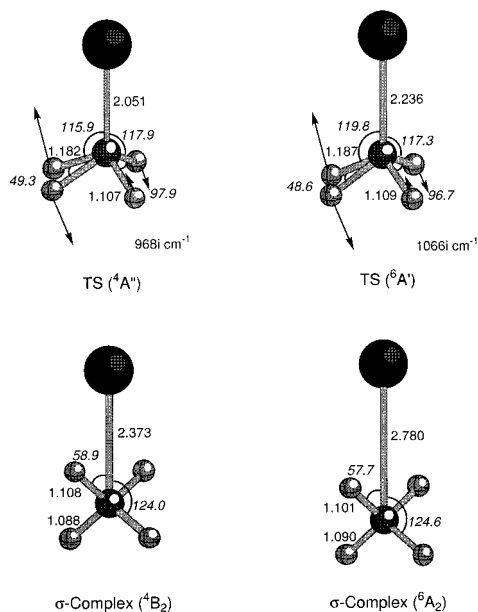


Figure 3. Optimized structures of the σ -complex (C_{2v}) and the transition state (C_s) for the inversion of methane on the $Fe^+(CH_4)$ complex. The bond distances are in angstroms, and the bond angles (italic) are in degrees. The arrows in the transition states indicate the transition vector.

spin state. The electron transfer from the methane to the Fe^+ ion resulting from the formation of the $Fe-C$ as well as the $Fe-H$ bonds plays a significant role in the activation of methane, as mentioned above.

Computed vibrational mode frequencies for free methane and the $Fe^+(CH_4)$ complex are listed in the Supporting Information. Agreement with experimental results is excellent for the vibrational frequencies, calculated wavenumbers of methane being accurate within a range of 1.7–3.6%. The conventional Hartree–Fock method in general overestimates molecular vibrational frequencies by typically 10%; this hybrid DFT method is therefore very useful for vibrational analyses. The 3-fold (T_2) and 2-fold (E) degenerate modes in T_d methane split into three and two bands, respectively, in the distorted C_{2v} structure (η^2 -H,H mode) of the $Fe^+(CH_4)$ complex. Such splitting is experimentally observable in the cobalt complex from measurements of FTIR matrix isolation spectroscopy.²¹ⁱ The main change in the vibrational modes of the $Fe^+(CH_4)$ complex is a slight downshift in wavenumber, but each degenerate mode of the complex exhibits a higher wavenumber than the value of the original degenerate mode.

The computed transition states for the Fe^+ complex have a C_s structure, in which one pair of C–H bonds is 1.182 (1.187) Å in length and the other pair is 1.107 (1.109) Å in the quartet (sextet) state. The bond angle of H–C–H for the long C–H pair is 49.3° (48.6°), and that for the short C–H pair is 97.9° (96.7°), in the quartet (sextet) state. Note that the $Fe-C$ distance is significantly decreased in the transition state compared to that in the σ -complex. The imaginary frequency of 1610i cm^{-1} for free methane is reasonably shifted down to 968i cm^{-1} in the quartet state and 1066i cm^{-1} in the sextet state. The downshift of frequency reasonably corresponds to the lowering of barrier height for the transition state. IRC analyses confirmed that the transition state correctly leads to the equivalent minimum in both the forward and reverse directions, as shown in Figure 4. Thus, the transition state shown in Figure 3 is, in fact, the true transition state for the inversion of methane at the Fe^+ active center. If such an alkane complex is formed as a

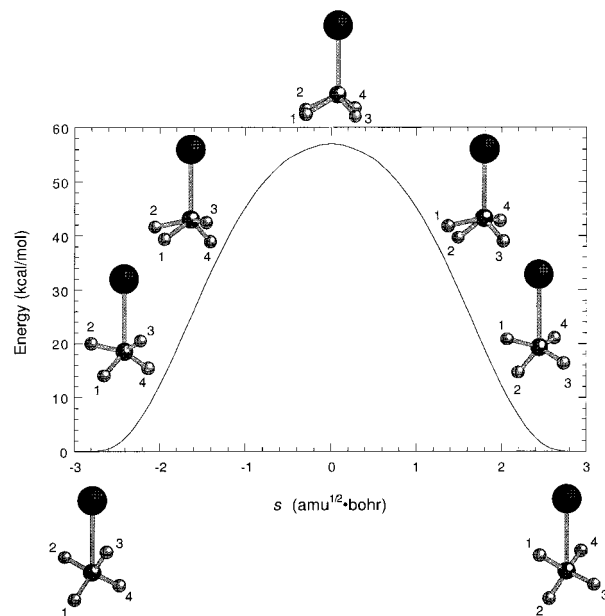


Figure 4. Energy profile and geometrical change along the intrinsic reaction coordinate (IRC) for the inversion of methane on the $Fe^+(CH_4)$ complex. Corrections of zero point vibrational energy are not included in the IRC analysis.

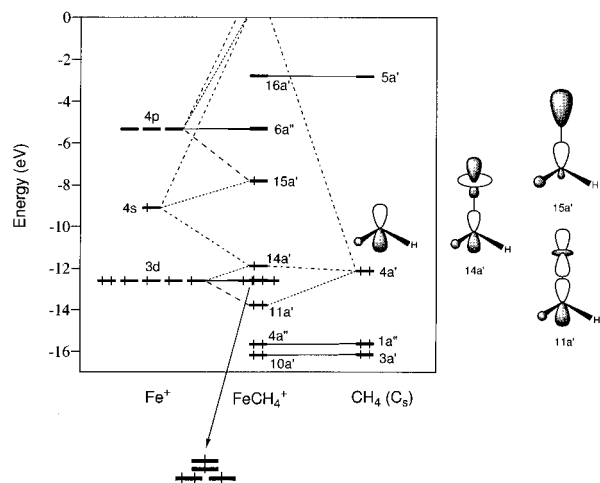


Figure 5. A fragment molecular orbital (FMO) analysis of the transition state for the inversion of methane on the $Fe^+(CH_4)$ complex. The spin state indicated is sextet.

reaction intermediate in C–H bond activation reactions, we expect that the inversion of alkane should reasonably occur, leading to loss of stereochemistry at a substrate carbon.

Fragment Molecular Orbital Analysis. To find a good reason why the barrier height for the inversion of methane is low on the low-spin states of the late transition-metal complexes $M^+(CH_4)$, we performed a fragment molecular orbital (FMO) analysis. Our method of choice is the extended Hückel method.² This approximate molecular orbital method should model general orbital energy trends and orbital interactions reasonably well. At the center of Figure 5, the molecular orbitals of the C_s transition state are constructed from the molecular orbitals of the Fe^+ and the CH_4 fragments. The 3-fold degenerate t_2 HOMO of methane splits into one at -12 eV and two at -16 eV, according to the distortion of methane. The HOMO at -12 eV interacts with one of the 3d orbitals of the Fe^+ ion, leading to the in-phase combination at -14 eV ($11a'$) and the out-of-phase counterpart at -12 eV ($14a'$), while the two orbitals of methane at -16 eV have no interaction with the Fe^+ ion. The in-phase

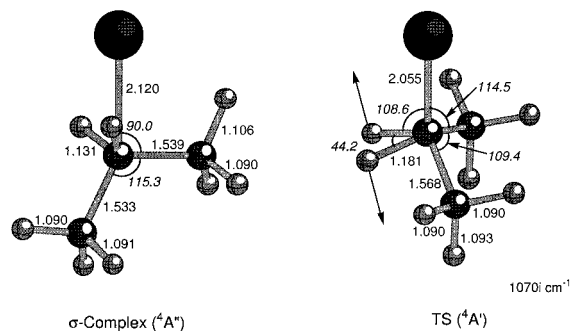


Figure 6. Optimized structures of the σ -complex (C_s) and the transition state (C_s) for the inversion of propane at the central carbon atom on the $\text{Fe}^+(\text{C}_3\text{H}_8)$ complex of the quartet state. The bond distances are in angstroms, and the bond angles (italic) are in degrees. The arrows in the transition states indicate the transition vector.

one is doubly filled, and the out-of-phase one singly filled. The $15a'$ orbital, which comes mainly from the $4s$ and $4p$ orbitals of the Fe^+ ion, lies 4 eV above the d -block orbitals around -12 eV.

The sextet and quartet states arise whether the $15a'$ orbital at -8 eV is filled or not, respectively. The quartet transition state lies 10 kcal/mol below the sextet transition state in the $\text{Fe}^+(\text{CH}_4)$ complex. Although explicit electron–electron interactions are not included in the extended Hückel method, we can gain some information about the preferred spin state from an empirical criterion within the framework of this one-electron theory; a low-spin state is expected in general to occur in the extended Hückel method if energy splitting between the two levels is more than 1.5 eV.²³ Therefore, the quartet transition state is predicted to lie below the sextet transition state because the high-lying $15a'$ orbital is vacant in the quartet state. By the same reasoning, the low-spin transition states of the $\text{Co}^+(\text{CH}_4)$, $\text{Ni}^+(\text{CH}_4)$, and $\text{Cu}^+(\text{CH}_4)$ complexes are more stable in energy than the corresponding high-spin transition states. Thus, such a one-electron picture is useful for the characterization of a transition state in considering what is energetically most stable among the possible spin states.

Propane Inversion on the $\text{Fe}^+(\text{C}_3\text{H}_8)$ Complex. It is interesting to look at how the inversion of other alkanes takes place in our stereoisomerization mechanism. Once H atoms of methane are replaced by bulky groups, the inversion pathway suggested by us will experience quite enhanced activation barriers. We therefore examined the inversion at the central carbon atom of propane on the $\text{Fe}^+(\text{C}_3\text{H}_8)$ complex. Figure 6 presents computed structures for the reactant complex and the transition state in the quartet state. Although we did not perform an IRC analysis for the reaction pathway, the imaginary mode of vibration ($1070i \text{ cm}^{-1}$) suggests that this saddle point is truly the transition state for the inversion of propane at the central carbon atom. The activation energy was computed to be 61.0 kcal/mol at the B3LYP level of theory. This enhancement in the activation energy is clearly due to the steric effect of the methyl groups. However, as mentioned earlier, this activation energy includes the binding energy of the $\text{Fe}^+(\text{C}_3\text{H}_8)$ complex (36.8 kcal/mol), the large binding energy being due to the two $\text{Fe}-\text{C}$ bonds and the two $\text{Fe}-\text{H}$ bonds. Therefore, the actual barrier height should be 24.2 kcal/mol if measured from the initial reactants Fe^+ and propane. We think that this transition state is also thermally accessible, as mentioned earlier in this paper.

(23) Hoffmann, R.; Zeiss, G. D.; Van Dine, G. W. *J. Am. Chem. Soc.* **1968**, *90*, 1485.

Inversion of Stereochemistry at the Substrate Carbon. Alkanes are in general considered to be among the most inert substrates for selective chemical functionalization. The so-called Fenton reaction²⁴ is a rare example of a successful hydroxylation of hydrocarbons using the $\text{Fe}^{2+}/\text{H}_2\text{O}_2$ system as a catalyst. In recent years there has been great interest in the C–H activation of small alkanes, particularly methane, in the hope of developing selective conversion of alkanes. Cytochrome P450²⁵ and soluble methane monooxygenase (MMO),²⁶ which involve iron–oxo species as active catalytic centers, are excellent biological catalysts for such a purpose, although P450 cannot hydroxylate methane. We should learn much from these enzymatic systems for developing man-made catalytic systems of high efficiency.

Accumulated studies have shown that P450- and MMO-catalyzed carbon hydroxylation reactions proceed with loss of stereochemistry. Stereochemical scrambling was first observed by Groves et al.²⁷ in the hydroxylation of *exo*-tetradeuterated norbornane by rabbit liver microsomes P450. Moreover, the hydroxylation of ethylbenzene by P450 was reported to proceed with 23–40% loss of stereochemistry.²⁸ Also in hydroxylation by soluble MMO, approximately 20–40% inversion of stereochemistry has been observed at labeled carbon atoms for alkane substrates.²⁹ The relatively high degree of inversion observed can be ascribed to flipping of a substrate intermediate that has a sufficiently long lifetime to undergo configurational inversion. It is thus generally believed that loss of stereochemistry requires a nonconcerted mechanism via a carbon radical as an intermediate species, because a carbon atom bearing an unpaired electron is planar. This radical mechanism is called “oxygen rebound mechanism”.²⁵

On the other hand, Newcomb and collaborators³⁰ have recently proposed a “nonsynchronous concerted” mechanism from measured, short radical lifetimes of less than 100 fs in both P450- and MMO-catalyzed hydrocarbon hydroxylations. They suggested that the widely believed hydroxylation mechanism, a radical mechanism, is incomplete or incorrect. Their proposed mechanism includes a side-on approach of oxygen to the C–H bond of the substrate as opposed to a linear C–H–OFe array of the conventional abstraction of an H atom. This description is essentially identical to the “oxenoid” model proposed many years ago by Hamilton³¹ and similar to the recent

(24) Recent reviews on Fenton-type reactions: Sawyer, D. T.; Sobokowiak, A.; Matsushita, T. *Acc. Chem. Res.* **1996**, *29*, 409. (b) Walling, C. *Acc. Chem. Res.* **1998**, *31*, 155.

(25) (a) *Cytochrome P450: Structure, Mechanism, and Biochemistry*, 2nd ed.; Ortiz de Montellano, P. R., Ed.; Plenum: New York, 1995. (b) Sono, M.; Roach, M. P.; Coulter, E. D.; Dawson, J. H. *Chem. Rev.* **1996**, *96*, 2841.

(26) (a) Wallar, B. J.; Lipscomb, J. D. *Chem. Rev.* **1996**, *96*, 2625. (b) Lipscomb, J. D. *Annu. Rev. Microbiol.* **1994**, *48*, 371. (c) Feig, A. L.; Lippard, S. J. *Chem. Rev.* **1994**, *94*, 759. (d) Lippard, S. J. *Angew. Chem., Int. Ed. Engl.* **1988**, *27*, 344. (e) Que, L., Jr.; Dong, Y. *Acc. Chem. Res.* **1996**, *29*, 190.

(27) Groves, J. T.; McClusky, G. A.; White, R. E.; Coon, M. J. *Biochem. Biophys. Res. Commun.* **1978**, *81*, 154.

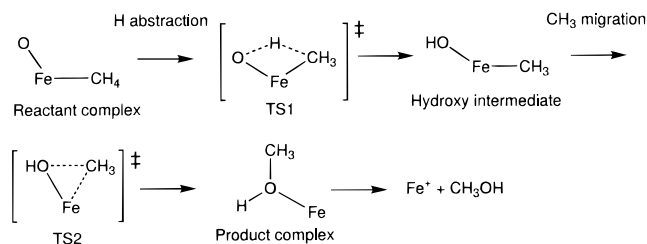
(28) White, R. E.; Miller, J. P.; Favreau, L. V.; Bhattacharyya, A. *J. Am. Chem. Soc.* **1986**, *108*, 6024.

(29) (a) Priestley, N. D.; Floss, H. D.; Froland, W. A.; Lipscomb, J. D.; Williams, P. G.; Morimoto, H. *J. Am. Chem. Soc.* **1992**, *114*, 7561. (b) Valentine, A. M.; Wilkinson, B.; Liu, K. E.; Komar-Panicucci, S.; Priestley, N. D.; Williams, P. G.; Morimoto, H.; Floss, H. G.; Lippard, S. J. *J. Am. Chem. Soc.* **1997**, *119*, 1818.

(30) (a) Newcomb, M.; Le Tadic-Biadatti, M.-H.; Chestney, D. L.; Roberts, E. S.; Hollenberg, P. F. *J. Am. Chem. Soc.* **1995**, *117*, 12085. (b) Choi, S. Y.; Eaton, P. E.; Hollenberg, P. F.; Liu, K. E.; Lippard, S. J.; Newcomb, M.; Putt, D. A.; Upadhyaya, S. P.; Xiong, Y. *J. Am. Chem. Soc.* **1996**, *118*, 6547. (c) Toy, P. H.; Dhanabalasingam, B.; Newcomb, M.; Hanna, I. H.; Hollenberg, P. F. *J. Org. Chem.* **1997**, *62*, 9114.

(31) Hamilton, G. A. In *Molecular Mechanism of Oxygen Activation*; Hayaishi, O., Ed.; Academic: New York, 1974.

Scheme 5

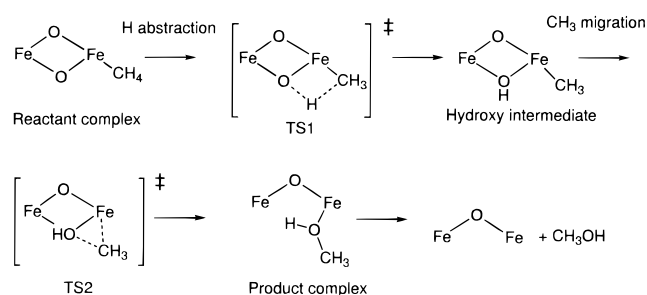


proposals of Shteinman for MMO hydroxylation³² and of Shestakov and Shilov for both P450 and MMO hydroxylations.³³ Recently, Collman *et al.*³⁴ proposed the reversible formation of an agostic complex between an alkane substrate and a high-valent iron-oxo species during the catalytic hydroxylation of hydrocarbons by P450 models.

We think that the key to understanding the catalytic and enzymatic hydrocarbon hydroxylations is in a simple gas-phase reaction. In 1990 Schröder and Schwarz³⁵ demonstrated that the bare FeO^+ complex, which is generated under ion cyclotron resonance conditions, converts methane to methanol in a high yield. In recent papers, we have theoretically proposed a “two-step concerted” mechanism for the methane–methanol conversion by the iron-oxo species³⁶ and by a diiron model of soluble MMO.^{22a,37} An important point of our proposal for the reaction pathway is that methane is activated on a coordinatively unsaturated iron-oxo species leading to a methane complex and that two-step concerted migrations of hydrogen and methyl successfully convert methane to methanol at the transition-metal active center, as indicated in Scheme 5. The transition states TS1 and TS2 were confirmed from detailed analyses of intrinsic reaction coordinate (IRC) to correctly connect the reaction pathway indicated. Our concerted mechanism is in good agreement with the experimental results of Schröder and Schwarz;^{35a} the barrier height of TS1 determines the reaction efficiencies of MnO^+ , FeO^+ , and CoO^+ and that of TS2 determines the methanol branching ratios.^{36b} Moreover, we showed that the concerted H atom abstraction via the four-centered TS1 is energetically more favorable than a direct H atom abstraction via a transition state with a linear C–H–OFe array.^{36c}

Various forms of soluble MMO have diiron structures on the active site.³⁸ We have applied the mechanism above to the methane hydroxylation by soluble MMO, but we have received a number of serious comments that the reactivity of the bare FeO^+ complex is essentially different from that of the active site of the diiron core of soluble MMO. However, as shown in Scheme 6, we recently demonstrated from DFT computations³⁷ that the conversion of methane to methanol can occur on a diiron

Scheme 6



model of intermediate **Q** of soluble MMO, which has been proposed to have an $\text{Fe}_2(\mu\text{-O}_2)$ diamond core,³⁹ in a way very similar to the gas-phase reaction indicated in Scheme 5. Ancillary ligands are not present in Scheme 6, but in our actual DFT computations four- and five-coordinate irons were assumed for the diiron model complex according to the report.³⁹ Our new concerted mechanism may lead to rejection or reinterpretation of the widely believed oxygen rebound mechanism for hydrocarbon hydroxylations by cytochrome P450 and soluble MMO.

The concerted mechanism was also successfully applied to a direct benzene hydroxylation by an iron-oxo species.⁴⁰ The reader may think that this mechanism is likely to always afford retention of stereochemistry at the carbon center of the substrate hydrocarbon. However, the inversion of methane can occur on the reactant σ -complexes in Schemes 5 and 6. Since the initial step of our concerted mechanism is the binding of methane to a coordinatively unsaturated transition-metal active center, the issue that we addressed in this paper should apply to the bare MO^+ complexes and the diiron analogue. We therefore expect that the inversion of methane should occur on such transition-metal-oxide complexes through a low-lying transition state to lead to the observed inversion of stereochemistry. If so, our two-step concerted mechanism would successfully explain the observed loss of stereochemistry that occurs in hydroxylations by the metalloenzymes. Thus, the radical mechanism (oxygen rebound mechanism)²⁵ may not be the sole source of the observed loss of stereochemistry in transition-metal-catalyzed reactions of hydrocarbons. We think that inversion of stereochemistry can reasonably occur in methane σ -complexes that we have proposed to be formed in the initial stages of the reaction between the substrate hydrocarbon and iron-oxo species of various forms.

Conclusions

The inversion of methane has been an important subject in theoretical chemistry since the original work of Hoffmann, Alder, and Wilcox. The purpose of this work is to shed new light on the potential meaning of this interesting subject. We discussed the inversion of methane on the $\text{M}^+(\text{CH}_4)$ complexes, in which M^+ is a first-row transition-metal ion from Sc^+ to Cu^+ . The methods we used are the B3LYP DFT method and the extended Hückel method. The transition states for the inversion of methane in these methane complexes appear to have an interesting C_s structure in which one pair of C–H bonds is about 1.2 Å in length and the other pair is about 1.1 Å. The activation barrier for the inversion of methane was computed to be 43–48 kcal/mol on the late transition-metal complexes

(32) (a) Shteinman, A. A. *Izv. Akad. Nauk. Ser. Khim.* **1995**, 1011. (b) Shteinman, A. A. *Russ. Chem. Bull.* **1995**, 44, 975. (c) Shteinman, A. A. *FEBS Lett.* **1995**, 362, 5.

(33) (a) Shestakov, A. F.; Shilov, A. E. *Zh. Obshch. Khim.* **1995**, 65, 60. (b) Shestakov, A. F.; Shilov, A. E. *J. Mol. Catal. A* **1996**, 105, 1.

(34) Collman, J. P.; Chien, A. S.; Eberspacher, T. A.; Brauman, J. I. *J. Am. Chem. Soc.* **1998**, 120, 425.

(35) (a) Schröder, D.; Schwarz, H. *Angew. Chem., Int. Ed. Engl.* **1990**, 29, 1433. (b) Schwarz, H. *Angew. Chem., Int. Ed. Engl.* **1991**, 30, 820.

(36) (a) Yoshizawa, K.; Shiota, Y.; Yamabe, T. *Chem. Eur. J.* **1997**, 3, 1160. (b) Yoshizawa, K.; Shiota, Y.; Yamabe, T. *J. Am. Chem. Soc.* **1998**, 120, 564. (c) Yoshizawa, K.; Shiota, Y.; Yamabe, T. *Organometallics* **1998**, 17, 2825.

(37) (a) Yoshizawa, K.; Ohta, T.; Shiota, Y.; Yamabe, T. *Chem. Lett.* **1997**, 1213. (b) Yoshizawa, K.; Ohta, T.; Yamabe, T. *Bull. Chem. Soc. Jpn.* **1998**, 71, 1899.

(38) (a) Rosenzweig, A. C.; Frederick, C. A.; Lippard, S. J.; Nordlund, P. *Nature* **1993**, 366, 537. (b) Rosenzweig, A. C.; Nordlund, P.; Takahara, P. M.; Frederick, C. A.; Lippard, S. J. *Chem. Biol.* **1995**, 2, 409.

(39) Shu, L.; Nesheim, J. C.; Kauffmann, K.; Münck, E.; Lipscomb, J. D.; Que, L., Jr. *Science* **1997**, 275, 515.

(40) Yoshizawa, K.; Shiota, Y.; Yamabe, T. *J. Am. Chem. Soc.* **1999**, 121, 147.

$\text{Fe}^+(\text{CH}_4)$, $\text{Co}^+(\text{CH}_4)$, $\text{Ni}^+(\text{CH}_4)$, and $\text{Cu}^+(\text{CH}_4)$. These values are much smaller than that for the inversion of free methane (109 kcal/mol) and the energy required for C–H bond cleavage of methane (104 kcal/mol). Therefore, such an inversion can reasonably occur at the transition-metal active center of catalysts and enzymes through a sufficiently low-lying transition state, leading to the observed inversion of stereochemistry at a carbon atom. We thus consider that a radical mechanism, the so-called oxygen rebound mechanism, may not be the sole source of the observed loss of stereochemistry in hydrocarbon hydroxylations and other related reactions catalyzed by transition-metal complexes and metalloenzymes. We should reconsider the origin of the observed inversion of stereochemistry.

Method of Calculation

We used the hybrid (density-functional-theory/Hartree–Fock) method of Becke¹⁸ and Lee, Yang, and Parr (LYP),¹⁹ the so-called B3LYP method, which consists of the Slater exchange, the Hartree–Fock exchange, the exchange functional of Becke,¹⁸ the correlation functional of LYP,¹⁹ and the correlation functional of Vosco, Wilk, and Nusair.⁴¹ The contribution of each energy to the B3LYP energy expression was fitted empirically on a reference set of molecules.^{18b} This hybrid method has been proposed to provide, in general, excellent descriptions of many reaction profiles, particularly in molecular geometries, heats of reaction, and activation energies of transition states.⁴² For the first-row transition metals we used the (14s9p5d) primitive set of Wachters⁴³ supplemented with one polarization f -function ($\alpha = 0.60$ for Sc, 0.69 for Ti, 0.78 for V, 0.87 for Cr, 0.96 for Mn, 1.05 for Fe, 1.17 for Co, 1.29 for Ni, and 1.44 for Cu)⁴⁴ resulting in a (611111111|51111|311|1) [9s5p3d1f] contraction, and for H and C atoms we used the 6-311G** basis set of Pople and co-workers.⁴⁵ Vibrational frequencies were systematically computed in order to ensure that on a potential energy surface all optimized geometries correspond to a local minimum that has no imaginary frequency or a saddle point that has only one imaginary

(41) Vosco, S. H.; Wilk, L.; Nusair, M. *Can. J. Phys.* **1980**, *58*, 1200.

(42) Baker, J.; Muir, M.; Andzelm, J.; Scheiner, A. In *Chemical Applications of Density-Functional Theory*; Laird, B. B., Ross, R. B., Ziegler, T., Eds.; ACS Symposium Series 629; American Chemical Society: Washington, DC, 1996.

(43) Wachters, A. J. H. *J. Chem. Phys.* **1970**, *52*, 1033.

(44) Raghavachari, K.; Trucks, G. W. *J. Chem. Phys.* **1989**, *91*, 1062.

(45) Krishnan, R.; Binkley, J. S.; Seeger, R.; Pople, J. A. *J. Chem. Phys.* **1980**, *72*, 650.

frequency. Zero point vibrational energy corrections were taken into account in calculating the total energies of the reactant (= product) complexes and the transition states. The spin-unrestricted method was applied to the open-shell systems. Computed $\langle S^2 \rangle$ values confirmed that spin contamination included in calculations was very small, within 0.3% after annihilation of spin contamination. These DFT computations were performed using the Gaussian 94 program package.⁴⁶ To draw a better picture for the interesting transition state, we performed orbital interaction analyses based on the extended Hückel method,² implemented with YAeHMOP.⁴⁷ The standard parameter set collected by Alvarez⁴⁸ was used in the present work, as indicated in ref 49.

Acknowledgment. This work was supported by a Grant-in-Aid for Scientific Research on the Priority Area Molecular Biometallics from the Ministry of Education, Science, Sports and Culture of Japan and by the Research for the Future Program from the Japan Society for the Promotion of Science (JSPS-RFTF96P00206). Computational time was provided by the Supercomputer Laboratory of Kyoto University and by the Computer Center of the Institute for Molecular Science.

Supporting Information Available: Table of computed vibrational frequencies of free methane and the $\text{Fe}^+(\text{CH}_4)$ complex (PDF). This material is available free of charge via the Internet at <http://pubs.acs.org>.

JA9839318

(46) Frisch, M. J.; Trucks, G. W.; Schlegel, H. B.; Gill, P. M. W.; Johnson, B. G.; Robb, M. A.; Cheeseman, J. R.; Keith, T. A.; Petersson, G. A.; Montgomery, J. A.; Raghavachari, K.; Al-Laham, M. A.; Zakrzewski, V. G.; Ortiz, J. V.; Foresman, J. B.; Cioslowski, J.; Stefanov, B. B.; Nanayakkara, A.; Challacombe, M.; Peng, C. Y.; Ayala, P. Y.; Chen, W.; Wong, M. W.; Andres, J. L.; Replogle, E. S.; Gomperts, R.; Martin, R. L.; Fox, D. J.; Binkley, J. S.; Defrees, D. J.; Baker, J.; Stewart, J. J. P.; Head-Gordon, M.; Gonzalez, C.; Pople, J. A. *Gaussian 94*; Gaussian Inc.: Pittsburgh, PA, 1995.

(47) Landrum, G. A. YAeHMOP “Yet Another extended Hückel Molecular Orbital Package”; version 2.0, Cornell University: Ithaca, New York, 1997.

(48) Alvarez, S. *Tables of Parameters for Extended Hückel Calculations*; Universitat de Barcelona, Barcelona, 1993.

(49) Parameters used for iron, carbon, and hydrogen atoms are Fe 4s ($H_{ii} = -9.1$ eV, $\zeta = 1.9$), Fe 4p ($H_{ii} = -5.32$ eV, $\zeta = 1.9$), Fe 3d ($H_{ii} = -12.6$ eV, $\zeta_{i1} = 5.35$, $c_1 = 0.5505$, $\zeta_{i2} = 2.00$, $c_1 = 0.6260$), C 2s ($H_{ii} = -21.4$ eV, $\zeta = 1.625$), C 2p ($H_{ii} = -11.4$ eV, $\zeta = 1.625$), and H 1s ($H_{ii} = -13.6$ eV, $\zeta = 1.3$), in which H_{ii} and ζ are the orbital energies and Slater exponents, respectively.